Fermi National Accelerator Laboratory

FERMILAB-Pub-86/64-A
February 1986

Percolation of Explosive Galaxy Formation

Jane C. Charlton and David N. Schramm

Astronomy and Astrophysics Center
The University of Chicago

Received 1986 February 19;

Abstract

A preliminary exploration is made of the possibility that at sufficiently high seed densities, explosive galaxy formation might percolate, thus losing the initial explosion scale. An assortment of parameter choices are investigated and the fractal patterns of the resultant systems are presented. It is shown that various dimension, d_f, fractal patterns, (power law correlation functions, $\xi(r) \sim r^{\gamma}$ with index $\gamma = d_f - 3$), can be obtained on scales which depend on the input. In particular, for one choice of parameters, it is possible to generate structure agreeing with galaxy-galaxy correlations out to $\sim 12 Mpc$. For another parameter choice, although the distribution generated is not as steeply correlated as galaxies are observed to be, a significant structure is generated on larger scales (out to $\sim 50 Mpc$). The models often produce a correlation function with a slope which changes in different distance ranges, thus a structure which is not entirely scale-free.

Subject headings: galaxies: clustering - galaxies: formation

I. Introduction

Ostriker-Cowie explosions (Ostriker and Cowie 1981) were proposed as a possible mechanism for galaxy formation, but isolated explosions of this type were only able to generate structure on very small scales. Here we will explore the question of whether explosions of primeval galaxies percolate (Schramm 1985), thus losing the initial explosion scale and allowing larger scale structure to be generated. One way of examining the plausibility of the percolating explosive galaxy formation mechanism is to compare the correlated structure it could produce to the observed two-point correlation function.

The distribution of galaxies and of clusters of galaxies can be described by the spatial two-point correlation function, $\xi_{12}(r)$. The galaxy-galaxy correlation function follows a power law out to distances of $\sim 15h^{-1}Mpc$, (h=$H_0/100$), beyond which it appears to be negative. This power law takes the form $\xi_{gg}(r)\approx 20(hr)^{-1.8}$ (Davis and Peebles 1983). The cluster-cluster correlation function for Abel richness ≥ 1 clusters can be approximated, (there is large uncertainty in the exponent), by the power law $\xi_{cc}(r)\approx 360(hr)^{-1.8}$ out to $\sim 150h^{-1}Mpc$ (Bahcall and Soneira 1983). The amplitude of the $R \geq 1$ cluster-cluster correlation function is thus $\sim$ 18 times higher than the galaxy-galaxy correlation function. It is, however, perhaps more natural to compare the amplitudes in terms of a dimensionless scale of units, in which r is divided by the mean separation between objects. In this system of units, galaxies are three times more strongly correlated than clusters of galaxies (Szalay and Schramm 1985). The power law behavior over a large range of distances and the relative constancy of the amplitude are indications of scale invariance. Thus, as with many phenomena in nature, it seems that the distribution of matter in the universe can be described as a fractal (Mandelbrot 1977) over a large range of distances. The fractal dimension, d_f, provides a description of the geometry of the distribution,

equivalent to the information provided by the exponent, γ, in the power law representation of the correlation function since the slope of the power law is simply $\gamma=d_f-3$. Thus we can think of the distribution of galaxies in space as a fractal of dimension $d_f=1.2$, an indication that some large scale structure exists since d_f is nowhere near the value of three that a uniform random distribution would produce. Although there is uncertainty in the observations, d_f also appears to be near 1.2 on the scale of clusters of galaxies (and maybe even superclusters (Bahcall 1985)). This brings about the question: what is the scale-free process which generates scale-invariant structure out to at least $15h^{-1}Mpc$ and provides correlations, if not continued scale-invariance, on even larger scales?

A potential candidate to explain the observed large-scale structure is a percolating (Schramm 1985) explosive galaxy formation mechanism. One such mechanism, based on the Ostriker-Cowie scenario, is described by Vishniac, Ostriker, and Bertschinger (1985). Here we use a closely related scheme. In this scheme, galaxy formation proceeds through an amplification of initial perturbations, which in this case are primeval galaxies with masses in the range 10^8–$10^{12}M_\odot$ and initial radii of 0.01–0.3Mpc, (when the value h=0.75 is used), at redshifts between fifty and two. These primeval galaxies explode with energies 10^{59}–$10^{63}ergs$, forming dense expanding shells behind a shock front. These large explosions are driven by explosions of many massive young stars within the galaxies. The shock waves are likely to initiate the formation of other primeval galaxies as they expand and intercept dense regions that we will call primordial galaxies, and provoke star formation in these regions. Thus later explosions of primeval galaxies are triggered by earlier events, resulting in a highly correlated network of material. If the network percolates to large enough distances and generates the correct correlation function, explosive galaxy formation could be the scale-free process required to match observations.

The model described in the previous paragraph differs in an important respect from the original Ostriker-Cowie scenario. They were concerned with the fragmentation of the shocked gas into gravitationally bound objects (which could then act as a second generation). In our model the seeds (primordial galaxies) are already present and require only an external pressure (triggering) to precipitate collapse and star formation.

A recent survey (Lapparent, Geller, and Huchra 1985) reveals that galaxies are distributed on the surfaces of shells surrounding voids with typical diameters of $25h^{-1}Mpc$. On first glance it seems that an explosive galaxy formation mechanism could naturally explain such structures.

It is important to realize that the two-point correlation function is far from being a complete description of the structure of the universe. Two different patterns with identical correlation functions can have significantly different features. Additional information is provided by three-point and four-point functions (Peebles 1980) that are observed to follow a simple hierarchical scaling pattern. Features such as filaments (Fry 1985a) and voids (Fry 1985b), that are clearly apparent to the eye, are often difficult to quantify statistically, but such details must be examined to obtain a complete analysis of a model. In this paper, however, we will concentrate on the two-point function as a first step towards examining the explosive galaxy formation model.

In section II, we discuss the method used to simulate galaxy formation and to determine the correlations of the resulting distribution of material. Section III is an application of these methods to a typical case. Section IV is a summary of the results and a discussion of the various trends in the data. In section V, we briefly examine the plausibility of this model in the real world, by relating its parameters to physical masses, distances, and times. We will see that the average radius of an explosion is at most $\sim 3Mpc$ and the average number density of

exploded galaxies is $\sim 0.01 Mpc^{-3}$. Section VI is a comparison of the most interesting cases to observations and a summary of results. Finally, in the Appendix, we tabulate all results.

II. Method

To simulate the distribution of material that would result from an explosive galaxy formation mechanism, we begin with n, (n=8000,16000 or 32000), locations of primordial galaxies within a cube with sides of unit length. These galaxies, which we will call "seeds", with Cartesian coordinates, x,y, and z, between 0 and 1, are randomly distributed. (Most simulations in percolation theory have been performed on a lattice.) Initially a fraction, f, of the seeds are randomly selected to represent the explosions, out to a radius r, of primeval galaxies in these locations. We designate these explosions as the first generation. It should be noted that, although these first generation explosions occur at the same time in this simulation, they would not realistically occur at the same time. It can be argued, however, that the time at which the explosions occur does not affect the eventual distribution of matter, and thus will not change the resulting fractal dimension. Any other explosions to occur in this simulation are "triggered" by previous explosions. Explosions are triggered at all those seed locations at distances less than r from any seed which has already exploded. Thus the first generation triggers any seeds which satisfy this distance criterion, and they form a second generation. The second generation members then trigger a third generation, the third a fourth, etc., until there are no seeds within a distance r of any seed which has been assigned to the last generation.

It should be noted that the use of a constant r is an approximation to simplify this simulation. Two effects, that tend to cancel, act to change r. First, explosions tend to be larger at later times due to dynamics considerations.

Second, the universe expands as the process occurs and the distance between seeds increases. This effect would not be important if the series of explosions takes place within a Hubble time, but it seems unlikely that this would be the case. A more detailed calculation would be required to determine the effects of a changing radius.

To assure that there are no edge effects, that would cause a deficiency of explosions near the edges of the cube, periodic boundary conditions are used, allowing explosions near one edge to trigger seeds on the opposite edges. Thus when calculating the distances between two seeds we use the minimum of x_2-x_1 , x_2-x_1+1, and x_2-x_1-1 as the separation in the x direction and the analogous minima as separations in the y and z directions.

Two parameters must be specified before a simulation run. It is convenient to express the first as the dimensionless ratio, D, of the radius of an explosion to the mean separation between seeds: $D=r/n^{-1/3}$. The second parameter is f, the fraction of the seeds exploding initially.

To obtain a completely scale-free structure the network of explosions must percolate, that is the largest interconnected network must extend to infinity or in our case from one edge of the cube to the other (Essam 1980). For our purposes it is adequate to make a rough judgement of whether percolation occurs. The members of the largest interconnected network are counted and identified. A three-dimensional diagram of this network alone can be examined to see if it extends through the entire space. Alternatively we can, in some cases, simply make the judgement based upon the number of members in the network, since if there are a very large number of members it may be obvious that percolation occurs.

A logarithmic plot of $N(r)$, (the number of pairs of points, among all the seeds which have exploded, in the bin at separation $r-\Delta r/2$ to $r+\Delta r/2$), vs. r is

examined. If the curve is flat in a certain range of r's, the distribution of matter is in a fractal pattern, over this range, with dimension, d_f, equal to the slope of the line. $N(r)$ is related to the two-point correlation function $\xi(r)$, by means of the equation:

$$\xi(r)=\frac{N(r)-N_{rand}(r)}{N_{rand}(r)}, \tag{1}$$

where $N_{rand}(r)$ is the number of pairs, in the bin at separation r, expected in a random distribution. The exponent, γ, in the power law correlation function is then simply given by: $\gamma=d_f-3$. To allow this plot to extend out to separations of 0.5 without edge effects, we must again calculate distances using periodic boundary conditions, as we did when setting up the distribution. We test the effectiveness of this procedure on a three-dimensional random distribution. This test yields $d_f=3.00$ as expected.

To be complete, we plot the same curve for the largest interconnected network alone when it has enough members that this is practical. It is not possible to avoid edge effects since a chain would not necessarily connect from one side to the opposite side if we were to use periodic boundary conditions. Instead we correct for edge effects, dividing $N(r)$ by a correction factor C where C is given by:

$$C=\frac{2}{\pi}\int_0^{\frac{\pi}{2}}\int_0^{\frac{\pi}{2}}(1-r\sin\theta\cos\phi)(1-r\sin\theta\sin\phi)(1-r\cos\theta)\sin\theta\,d\theta\,d\phi$$
$$=1-1.5r+0.63662r^2-0.079577r^3 \tag{2}$$

This correction is verified to yield a plot with slope 3.00 when applied to a random distribution. Corrected and uncorrected curves are presented in Figure 1 for $n=8000$ randomly distributed points.

The above methods will be illustrated by the example in the following section.

III. Sample Case

A typical case which illustrates all the methods described in the previous section is the case with D=0.8 and f=0.02. For this case it is most convenient to choose n=16000, since for this value a large enough number of seeds explode to accurately determine the correlation function. $f \times n$=320 of these seeds explode initially. Three runs are executed, each with different random coordinates chosen as seed locations. We discuss here the results for what we denote as run a. In run a the 320 first generation explosions trigger 659 second generation explosions. This process continues until 4004 seeds have exploded. The shells of these explosions are illustrated in Figure 2a. In this figure no non-random structure is readily apparent. The longest interconnected network among the 4004 explosions has 2491 members. This network alone is plotted in Figure 2b. Next, the curve $\log N(r)$ vs. $\log r$, given in Figure 3, is examined. The slope of the curve increases as we pass from lower to higher separations as might be expected. There is a flat portion of the curve, with slope d_f=2.01±.02, between $1.1r_e$ and $2.4r_e$ where r_e is the radius of an explosion:

$$r_e = Dn^{-1/3} = 0.03175. \tag{3}$$

The slope of the correlation function, γ, in this region is then –0.99±.02. The region of the curve between $2.5r_e$ and $6.6r_e$ has an average slope of 2.55±.02, yielding γ=–0.45±.02, and the region between $6.9r_e$ and $14.4r_e$ gives d_f=3.09±.01 or γ=+0.09±.01. This increase in slope to near three at higher separations is typical to many cases. It can be understood in the case D=0.08, f=0.02 by observing that the average number of generations triggered successively by a first generation member is 12.5 so that when we look at scales larger than some fraction of $12.5r_e$ we might expect a random distribution. The slope of three at large separations also explains the lack of observable structure in Figure 2a. The largest network of explosions for D=0.8, f=0.02 is found to have a

slope d_f=2.23±.01, so that γ=-0.77±.01, from $1.3r_e$ to $7.7r_e$.

To facilitate comparison of models with the same D and f, but with a different initial distribution of seeds, in Table 1 we present results for three runs of the case with D=0.8, f=0.02. Note that although the parameters D and f are the same, the results are quite different in cases a,b, and c.

IV. Results and Trends

The cases of interest have a D between 0.5 and 0.9. For a lower value of D explosions are too small, compared to the seed separation, to detonate others so the final distribution is very similar to the initial random distribution. If, instead, D is larger than 0.9 almost all of the seeds explode so, again, the result is a nearly random distribution. For each value of D, several values of f are of interest; the larger the value of D, the smaller the f required to achieve percolation.

A table of results is presented in the Appendix. Here we will summarize these results by pointing out the trends that exist. Figures 4 a,b, and c illustrate, for assorted values of D and f, the slopes of the correlation function, γ, and the scales over which they apply. Each of the three diagrams depicts cases with a different initial random distribution of seeds. It can be seen that the highest correlations, that is the largest negative values of γ for a given D and f, usually occur on the smallest scales and apply only out to about $4r_e$ on the average. Beyond this separation the slope of the correlation function increases gradually to a value of approximately zero in most cases. The limited range of applicability could be anticipated, since beyond a certain distance, $\sim 4r_e$, chains of triggered explosions tend to branch off in all directions thus increasing the fractal dimension. The nearly uncorrelated, γ=0, structure at large separations can be understood, since on larger scales we can imagine isolated randomly distributed clumps

of explosions, with each clump containing explosions which were ultimately triggered by a certain set of first generation explosions.

Keeping in mind that the correlation functions have a constant slope only over the limited separation ranges illustrated in Figure 4, Figure 5 better facilitates the comparison of the γ's at the smallest separation range. We notice several trends. First, γ approaches 0 for D=0.5 and D=0.9 for the reasons described above. But in between these values we see increased correlations since explosions are large enough to encompass some seeds, but not so large as to detonate too many of them. We also see that for a constant D, the degree of correlation decreases with increasing f. This can be understood since, the more explosions that are ultimately triggered by each first generation member, the more correlated the resulting pattern. The average number of triggers per first generation member is usually larger if there are fewer first generation members, as can be seen in the Appendix.

The values of γ for the largest interconnected networks are not presented here since they are not central to the point of this paper; however, they are tabulated in the Appendix for reference.

V. Relation to the Universe

To make a judgement as to whether the models of galaxy formation that we have considered are capable of producing the observed structure of the universe, we must relate them to physical distances and densities. First of all the size of an explosion must be estimated. Then we will see if the cases of interest require realistic mass densities in seeds, that is mass densities lower than the total baryon density of the universe. Finally, we consider whether the detonation process proceeds rapidly enough to allow a substantial number of successive triggers within a reasonable time scale.

The maximum radius of an explosion, that is still capable of detonating a seed, can be estimated using the Sedov solution (Sedov 1959; Schwartz, Ostriker, and Yahil 1975; Bertschinger 1983) which describes the self-similar expansion of the shock during the adiabatic phase:

$$R=1.1\left(\frac{E}{\rho_e}\right)^{1/5}t^{2/5}. \tag{4}$$

For t we substitute the gravitational timescale, that is the Hubble time when the explosion occurred. After this time, compressional effects of the shock on an intercepted seed are weak, so the seeds will not form primeval galaxies and detonate. (The Hubble time is a reasonable choice for cutoff only in the compressional hypothesis. Fragmentation of a shock wave, as would be necessary in the original Ostiker-Cowie scheme, actually becomes easier as the age of the shock approaches the age of the universe (Vishniac, Ostriker, and Bertschinger 1985).) For ρ_e we use the density of the universe at the redshift of interest:

$$\rho_e=1.9\times10^{-29}h^2\Omega(1+z)^3 g/cm^3.$$

We write t in terms of the present age of the universe, t_0, and the redshift, z_i, at which the explosion occurred:

$$t=t_0(1+z_i)^{-3/2}. \tag{6}$$

Using the value $t_0=1.5\times10^{10}$ years, we obtain

$$R=3.93(h^2\Omega)^{-1/5}(1+z_i)^{-6/5}E_{61}^{1/5}Mpc \tag{7}$$

or in comoving coordinates

$$R=2.47(h^2\Omega)^{-1/5}(1+z_i)^{-1/5}E_{61}^{1/5}Mpc. \tag{8}$$

It has been shown (Sato and Maeda 1983; Ikeuchi, Tomisaka, and Ostriker 1983) that void regions in the universe expand faster than the outer unperturbed comoving regions. Specifically, in a closed universe, $R\sim t^{4/5}$. Thus the void has an additional growth by a factor $(1+z)^{1/5}$ and the radius of the explosion today is given by:

$$R=2.47(h^2\Omega)^{-1/5}E_{61}^{1/5}Mpc=2.77Mpc \tag{9}$$

if the values $\Omega=1$, $h=0.75$, and $E_{61}=1$ are used. Thus the maximum plausible radius for an explosion is $\sim 3Mpc$. (This is much smaller than the limit of $20Mpc$ provided by microwave background radiation constraints (Vishniac and Ostriker 1985), and is also smaller than the shells on which galaxies have recently been observed (Lapparent, Geller, and Huchra 1985)). It is apparent that this result is not highly dependent on our choices of E, t_0, h and Ω. Thus when we have a fractal dimension applicable out to $4r_c$, this is only at most $12Mpc$, a small scale compared to observations.

Although the result for the maximum radius of an explosion is not highly dependent upon the energy of the explosion, it is still worthwhile to consider maximum energy constraints. Discussions of this question are given in Wandel (1985) and in Vishniac, Ostriker, and Bertschinger (1985). During the Compton cooling epoch, at redshifts greater than approximately 11, the maximum energy is given by:

$$E_{61}=7.6\times 10^8\epsilon_{-4}^{5/2}(h^2\Omega)^{1/4}(1+z)^{-21/4}f_I \tag{10}$$

where ϵ is the efficiency and f_I is the fraction of matter contained in interstellar gas. At $z=50$ this limit is on the order of $E_{61}\sim 1$, and at $z=30$ it has increased to $E_{61}\sim 10$. The upper bound on the energy allowed in an explosion continues to increase, perhaps by another order of magnitude, until the redshift at which radiative cooling begins to dominate Compton cooling. At these lower redshifts a reasonable estimate of the explosion energy is the energy a very young galaxy might inject into the intergalactic medium, typically $E_{61}\sim 1$. Thus the energy can never greatly exceed the value, $E_{61}=1$, that we have used in our radius estimate, so the value of R cannot be significantly larger.

$D=0.5$–0.9 and $R=3Mpc$ correspond to a number density of primeval galaxies of 0.005 - 0.03 Mpc^{-3}. Assuming that mass of a primeval galaxy is in the

range 10^8-$10^{12}M_\odot$, the mass density of primeval galaxies is between 3.3×10^{-35} and $2.0\times10^{-30}g/cm^3$. The baryon density of the universe , even as late as z=2, is $\geq 9\times10^{-30}g/cm^3$. Thus the densities required, for the cases we have examined here, are safely under the critical density.

Next we focus on the question of the timescale. If it is assumed that detonation of each new generation occurs after one Hubble time, we find

$$t_f=2^{(n-1)}t_i \tag{11}$$

where n is the number of generations and t_i and t_f are the initial and final times. If we begin at z=50, we can fit in only seven generations before z=2, even having overestimated the time before detonation. If, instead, triggering was to occur after the Compton cooling time had elapsed, sixty generations could occur between z=50 and z=11, but the radius of these explosions would be smaller. It is clear, however, that some of the cases we have examined, (those with a large average number of triggers), could have later generations cut off due to this time constraint, and thus may not be realistic.

VI. Conclusion

We conclude with a discussion of what might be considered the most interesting cases, the one with the largest correlations and the one which has correlations out to the largest scales.

The case with D=0.75 and f=0.01 has the most highly correlated structure of the cases we have considered. Three runs of this case gave $\gamma=-1.72\pm.03$ out to $3.2r_e$, $\gamma=-1.67\pm.03$ out to $4.3r_e$, and $\gamma=-1.84\pm.03$ out to $3.2r_e$. On first glance, this case does look promising since the slope of the correlation function is nearly identical to the observational value of $\gamma=-1.8$. But we must recall that 3 - 4 r_e is only 9 - 12 Mpc at most, not a large enough scale to explain the galaxy-galaxy correlations out to $\sim$ 15Mpc, and certainly nowhere near the scale of

cluster-cluster correlations. It should be noted that the slope of the plot of $\log N(r)$ vs. $\log r$ increases gradually to three, corresponding to $\gamma=0$, a value it reaches at 6 - $7r_e$. As we would expect an illustration, given in Figure 6, of the distribution of matter appears random, as did the distribution in Figure 2a.

Although the correlations in the case $D=0.85$, $f=0.0005$ are not large enough to match observations, even on the smallest scales, it still has the advantage of significant correlations on larger scales. The curves $\log N(r)$ vs. $\log r$ for runs a,b, and c are given in Figure 7. The values of γ for the various separation ranges are listed in Table 2. We notice in all three runs, a decreasing slope, of the curve $\log N(r)$ vs. $\log r$, with increasing separations out to at least $9r_e$, behavior opposite to the usual trend. The structure is actually more highly correlated at large separations. In run c, the slope never reaches three, but continues to decrease out to $17.1r_e$, the maximum separation considered. In this run, γ is between -1.21 and -0.77 in the entire range of separations. Figure 8 illustrates the distribution of material in run c. Here we see two separate structures as well as several smaller ones. We can see that structure has been generated, even on large scales, in contrast to featureless Figure 2a and the distribution produced in the case $D=0.75$, $f=0.01$. It should be noted that run c of the case with $D=0.85$, $f=0.001$ exhibits similar behavior, with a γ in the range between -0.94 and -0.66. Although the γ's in these cases are not as low as the observed $\gamma=-1.8$, significant structure is generated on large scales. These cases could, however, be unrealistic due to time constraint considerations since more than 100 average successive triggers are required.

An interesting feature of nearly all cases is a correlation function with a slope that changes in different ranges of separations. In most cases we find a trend towards lower d_f, shallower correlation functions, at larger separations, although we have also discussed a case in which d_f decreases at larger separations.

Thus it could be said that an observed trend of a correlation function with changing slope on larger scales would support this method for generating structure. This contradicts the preliminary indications of Bahcall and Soneira (1983).

It is quite possible that gravitational evolution could change the slope of the correlation function, or it could change the standard model, as studied numerically by Davis, Efstathiou, Frenk, and White (1985).

Although the simple model we have used here to simulate explosive galaxy formation does not succeed in generating the observed structure of the universe, it does have certain advantageous features. For certain cases it has been possible to generate structure with a fractal dimension as low as 1.2, that is a $\gamma \sim -1.8$, if only on very small scales. Perhaps, the most significant result is the possibility, for other cases, of generating highly correlated structure out to the largest separations that we consider. This certainly provides grounds for further explorations. Perhaps the assumption of a Gaussian initial distribution is unrealistic (Peebles 1983). If we were to begin with an already correlated distribution, for example, a cold particle distribution, the result could be a distribution with an even lower fractal dimension. Another possibility is an initial distribution of seeds in pancakes so that the percolated structures have constrained domains. It seems quite possible that some variation of the percolating explosive galaxy formation mechanism described here is an element of the process that generated the observed correlated large scale structure.

Acknowledgements

We would like to thank A. Melott for many stimulating conversations, for assistance in computing, and for reviewing this manuscript. We are also grateful to J. Fry, A. Königl, I. Procaccia, P. Shapiro, A. Szalay, and L. Widrow for their apt suggestions, and to P. Schinder for providing learned guidance in the construction of the computer code. The comments of the referee, E. Vishniac, were especially pertinent.

We would like to acknowledge computer time on the Cray XMP at the National MFE Computing Center at Livermore as sponsored by the astrophysics group at Fermilab and on the University of Chicago Department of Astronomy and Astrophysics Vax that is supplemented by the William Gaertner fund. This material is based on research supported by the NSF under grant number AST 8313128 and by DOE grant DE-AC02-80ER10773 A004.

Table 1: Sample Case Results[a]

# exp.	γ	Range (r_e)	γ	Range (r_e)	γ	Range (r_e)	#lar. net.	$\tilde{\gamma}$	Range (r_e)
4004	-0.99±.02	1.1-2.4	-0.48±.02	2.5-6.6	+0.09±.01	6.9-14.4	2491	-0.77±.01	1.3-7.7
4217	-0.89±.02	1.1-3.0	-0.37±.02	3.2-6.0	0.00±.006	6.3-14.4	3031	-0.76±.02	1.3-4.1
5095	-0.82±.02	1.1-2.6	-0.33±.02	2.7-6.0	-0.05±.003	6.3-14.4	4124	-0.72±.01	1.3-3.7

[a]This table contains results for the example case with D=0.8, f=0.02. For the three runs of this case, each with a different random initial distribution of seeds, we give the number of the 16000 initial seeds that explode, the values of γ and the separation ranges in which they apply, the number of members in the largest interconnected network and the value of γ for this network in the specified separation range.

Table 2: Correlation Properties[a]

Run	# exp.	γ	Range (r_σ)	γ	Range (r_σ)	γ	Range (r_σ)	γ	Range (r_σ)
a	2979	-0.67±.02	1.1-3.1	-1.04±.02	3.3-5.9	-1.68±.02	6.1-9.1	-0.18±.04	11.6-17.1
b	6251	-0.67±.01	1.1-5.3	-0.76±.01	5.6-9.5	-0.04±.02	11.0-17.1		
c	2230	-0.77±.03	1.1-2.4	-1.08±.005	2.6-11.6	-1.21±.04	12.2-17.1		

[a]Correlation properties of the noteworthy case with D=0.85, f=0.0005.

Appendix

Table 3: Model Parameters[a]

D	f	n	# exp.	Av. trig.	γ	Range (r_g)	γ	Range (r_g)	γ	Range (r_g)	#bar. net.	γ	Range (r_g)
0.6	0.2	8000	2392	1.5	-0.91± .33	1.1-1.7	+0.001± .006	3.2-18.3			41		
0.6	0.2	8000	2363	1.5	-0.58± .12	1.1-1.9	-0.004± .004	3.2-18.3			25		
0.6	0.2	8000	2405	1.5	-0.45± .06	1.1-3.0	+0.001± .005	3.2-18.3			20		
0.6	0.5	8000	5072	1.3	-0.01± .005	1.1-18.3					235		
0.6	0.5	8000	4982	1.3	-0.02± .004	1.1-18.3					285		
0.6	0.5	8000	5049	1.3	-0.01± .003	1.1-18.3					266		
0.6	0.2	8000	3091	1.9	-0.45± .06	1.1-3.4	+0.014± .006	3.5-15.2			183		
0.6	0.2	8000	3075	1.9	-0.37± .04	1.1-3.7	+0.004± .003	3.9-15.2			226		
0.6	0.2	8000	3160	2.0	-0.42± .04	1.1-3.4	+0.005± .004	3.5-15.2			234		
0.6	0.5	8000	5742	1.4	-0.013± .004	1.1-15.2					5420	-0.022± .003	1.8-31.7
0.6	0.5	8000	5678	1.4	-0.025± .005	1.1-15.2					5341	-0.027± .004	1.8-31.7
0.6	0.5	8000	5689	1.4	-0.016± .004	1.1-15.2					5420	2.975± .003	1.8-31.7
0.7	0.05	16000	3384	4.2	-1.38± .05	1.1-2.2	-0.007± .006	3.2-13.1			145		
0.7	0.05	16000	3558	4.4	-1.25± .03	1.1-2.5	0.000± .004	2.9-13.1			141		
0.7	0.05	16000	3581	4.5	-1.26± .04	1.1-2.3	+0.006± .006	3.5-13.1			214		
0.7	0.1	8000	2755	3.4	-0.89± .03	1.1-2.5	-0.015± .005	3.2-13.1			1373	-0.54± .03	1.5-5.2
0.7	0.1	8000	2867	3.5	-0.83± .03	1.5-2.7	+0.005± .005	3.7-13.1			1701	-0.59± .02	1.5-4.5
0.7	0.1	8000	2839	3.6	-0.77± .03	1.1-2.7	-0.004± .006	3.2-13.1			929	-0.58± .01	1.5-12.5
0.7	0.2	8000	4326	2.7	-0.34± .03	1.1-2.9	+0.002± .002	3.0-13.1			4173	-0.033± .003	2.0-22.4
0.7	0.2	8000	4351	2.7	-0.36± .04	1.1-2.7	-0.008± .004	2.9-13.1			4150	-0.033± .005	2.0-19.8
0.7	0.2	8000	4336	2.7	-0.40± .03	1.1-2.4	+0.004± .006	2.5-13.1			4127	-0.045± .004	2.0-18.4
0.75	0.01	32000	2880	9.0	-1.72± .03	1.2-3.2	-0.77± .08	3.7-4.9	-0.03± .01	5.5-19.4			
0.75	0.01	32000	3124	9.8	-1.67± .08	1.1-4.3	+0.07± .01	6.6-19.4					
0.75	0.01	32000	2713	8.5	-1.84± .05	1.3-3.2	+0.10± .01	8.1-19.4					
0.75	0.02	16000	2306	7.2	-1.38± .02	1.1-3.2	+0.04± .01	5.3-15.4			155		
0.75	0.02	16000	2457	7.7	-1.35± .05	1.3-2.8	-0.09± .01	4.3-15.4			357		
0.75	0.02	16000	2608	8.2	-1.40± .05	1.2-2.7	+0.01± .01	5.5-15.4			253		
0.75	0.05	16000	4867	6.1	-1.01± .03	1.1-2.3	-0.33± .04	2.4-3.7	-0.013± .004	3.9-15.4	3340	-1.04± .04	1.4-2.2
0.75	0.05	16000	5139	6.4	-0.93± .04	1.1-2.1	-0.47± .04	2.9-3.6	+0.009± .004	3.7-15.4	4031	-0.83± .02	1.4-3.2
0.75	0.05	16000	5105	6.4	-0.98± .03	1.1-2.4	-0.30± .03	2.5-3.7	-0.024± .004	3.9-15.4	2607	-0.53± .01	1.5-6.4
0.8	0.005	32000	3892	21.2	-1.13± .01	1.1-6.5	+0.13± .02	12.9-18.2					
0.8	0.005	32000	3854	21.0	-1.21± .01	1.1-5.4	+0.13± .03	12.3-18.2					
0.8	0.005	32000	2708	18.0	-1.53± .01	1.1-4.9	+0.05± .01	7.6-18.2					
0.8	0.005	16000	1051	13.1	-1.55± .02	1.6-4.9	+0.26± .04	9.3-13.1			90		
0.8	0.005	16000	1585	19.8	-1.40± .02	1.3-4.5	-0.02± .02	8.0-14.4			295		
0.8	0.005	16000	1641	20.5	-1.32± .02	1.4-3.7	+0.22± .07	11.3-14.4			138		
0.8	0.01	16000	2371	14.8	-1.12± .01	1.1-4.7	+0.14± .02	8.4-14.4			323		
0.8	0.01	16000	2637	16.5	-1.09± .02	1.1-4.5	-0.02± .01	6.6-14.4			510		
0.8	0.01	16000	3360	21.0	-0.91± .01	1.1-4.1	-0.08± .01	8.0-14.4			808		

D	f	n	# exp.	Av. trig.	γ	Range (r_c)	γ	Range (r_c)	γ	Range (r_c)	# lar. net.	γ	Range (r_c)
0.8	0.02	16000	4004	12.5	-0.99± .02	1.1-2.4	-0.48± .02	2.5-6.6	+0.09± .01	6.9-14.4	2491	-0.77± .01	1.3-7.7
0.8	0.02	16000	4217	13.2	-0.89± .02	1.1-3.0	-0.37± .02	3.2-6.0	-0.003± .006	6.3-14.4	3031	-0.76± .02	1.3-4.1
0.8	0.02	16000	5095	15.9	-0.82± .02	1.1-2.6	-0.33± .02	2.7-6.0	-0.052± .003	6.3-14.4	4124	-0.72± .01	1.3-3.7
0.8	0.05	8000	3623	9.1	-0.70± .04	1.1-2.2	-0.15± .02	2.3-5.5	+0.03± .01	5.8-11.5	3515	-0.51± .03	1.3-3.4
0.8	0.05	8000	3703	9.3	-0.64± .04	1.1-2.1	-0.20± .01	2.2-5.0	+0.001± .005	5.2-11.5	3563	-0.39± .02	1.2-3.4
0.8	0.05	8000	3700	9.3	-0.67± .03	1.1-2.3	-0.25± .03	2.4-4.1	+0.035± .005	4.3-11.5	3575	-0.60± .03	1.3-3.4
0.85	0.0005	32000	2979	186	-0.67± .02	1.1-3.1	-1.69± .02	6.1-9.1	-0.18± .04	11.6-17.1			
0.85	0.0005	32000	6251	391	-0.67± .01	1.1-5.3	-0.76± .01	5.6-9.5	-0.04± .02	11.0-17.1			
0.85	0.0005	32000	2230	139	-0.77± .03	1.1-2.4	-1.08± .005	2.6-11.6	-1.21± .04	12.2-17.1			
0.85	0.001	32000	5172	162	-0.71± .01	1.1-6.1	-0.11± .01	10.0-17.1					
0.85	0.001	32000	7835	245	-0.63± .004	1.1-9.1	+0.03± .01	11.0-17.1					
0.85	0.001	32000	2891	90.3	-0.94± .02	1.1-4.2	-0.66± .01	10.0-17.1					
0.85	0.001	16000	1322	82.6	-0.97± .02	1.5-4.6	-1.25± .01	4.8-13.6			484		
0.85	0.001	16000	1236	77.3	-0.98± .02	1.7-4.0	-1.32± .01	4.8-13.6			484		
0.85	0.001	16000	3595	135	-0.60± .004	1.1-13.6					1650	-0.45± .01	1.2-6.9
0.85	0.002	16000	2799	87.5	-0.66± .005	1.7-13.6					1834	-0.697± .004	1.2-11.7
0.85	0.002	16000	2344	73.3	-0.88± .01	1.1-6.5					1647	-0.668± .008	1.2-7.9
0.85	0.002	16000	4307	225	-0.59± .01	1.1-4.6					2046	-0.451± .006	1.2-7.6
0.85	0.005	16000	4390	54.9	-0.61± .01	1.1-5.4	-0.13± .01	9.2-13.6			3807	-0.55± .01	1.2-9.7
0.85	0.005	16000	4758	59.5	-0.68± .01	1.2-4.6	-0.03± .01	7.2-12.9			3848	-0.61± .01	1.2-5.4
0.85	0.005	16000	5677	71.0	-0.55± .01	1.1-3.6	-0.23± .01	5.4-13.6			5472	-0.53± .01	1.2-3.6
0.9	0.0005	8000	5834	1459	-0.30± .03	1.1-1.8	-0.002± .005	1.9-10.2			5831	-0.047± .005	1.4-14.3
0.9	0.0005	8000	5900	1475	-0.22± .03	1.1-1.9	-0.048± .005	2.0-10.2			5898	-0.044± .004	1.3-14.3
0.9	0.0005	8000	5566	1391	-0.29± .02	1.1-2.0	-0.074± .005	2.1-10.2			5558	-0.153± .005	1.3-9.2
0.9	0.001	8000	5834	729	-0.07± .01	1.4-10.2					5831	-0.041± .003	1.6-21.2
0.9	0.001	8000	5910	739	-0.07± .01	1.4-10.2					5908	-0.052± .004	1.2-15.8
0.9	0.001	8000	5586	698	-0.08± .01	1.8-10.2					5559	-0.121± .007	1.3-13.6

[a]This table is a presentation of results for cases with various choices of the parameters D and f. Each of the three cases in a group has the same D, f and n, but a different random initial distribution of seeds. # exp. is the number of the n initial seeds that ultimately explode and av. trig. is the average number of seeds triggered by each first generation member. Columns 6-11 tabulate the slope, γ, of the correlation function in the ranges of separations in which this slope is relatively constant. The last three columns contain the number of members in the largest interconnected network, the values of γ for the network, and the range in which these values apply. In some cases the largest network does not have a large enough number of members to allow us to investigate its correlations. For the several cases where there is no entry for the number of members in the largest interconnected network, the number is clearly quite small.

References

Bahcall, N. A. 1985, preprint.

Bahcall, N. A. and Soneira, R. M. 1983, *Ap. J.*, **270,** 20.

Bertschinger, E. 1983, *Ap. J.*, **268,** 17.

Davis, M., Efstathiou, G., Frenk, C. S. 1985, *Ap. J.*, **292,** 371.

Davis, M. and Peebles, P. J. E. 1983, *Ap. J.*, **267,** 465.

Essam, J. W. 1980, *Rep. Prog. Phys.*, **43,** 833.

Fry, J. N. 1985a, preprint.

Fry, J. N. 1985b, preprint.

Mandelbrot, B. 1977, *Fractal Symmetry of Nature* (Freeman: San Francisco).

Ostriker, J. P. and Cowie, L. L. 1981, *Ap. J.*, **243,** L127.

Peebles, P. J. E. 1983, *Ap. J.*, **274,** 1.

Peebles, P. J. E. 1980, *The Large Scale Structure of the Universe* (Princeton Univ. Press: Princeton).

Sato, H. and Maeda, K. 1983, *Prog. Theor. Phys.*, **70,** 1.

Satora, I., Tomisaka, K., and Ostriker, J. P. 1983, *Ap. J.*, **265,** 583.

Schramm, D. N. 1985, in *Proceedings, 3rd Rome Conf, Nouvo Cimento*, in press.

Schwartz, J., Ostriker, J. P., and Yahil, A. 1975, *Ap. J.*, **202,** 1.

Sedov, L. I. 1959, *Similarity and Dimensional Methods in Mechanics* (Academic Press: New York).

Szalay, A. S. and Schramm, D. N. 1985, *Nature*. **314,** 718.

Vishniac, E. T., Ostriker, J. P. and Bertschinger, E. 1985, *Ap. J.*, in press.

Vishniac, E. T. and Ostriker, J. P. 1985, preprint.

Wandel, A. 1985, *Ap. J.*, **294,** 385.

Figure Captions

Figure 1:

Corrected and uncorrected curves of $\log N(r)$ vs. $\log r$ for n=8000 randomly distributed points, demonstrating the validity of the edge effects corrections that were applied when calculating this same curve for the largest interconnected networks. (It was not necessary to apply such corrections when it was possible to use the periodic boundary conditions described in the text.)

Figure 2:

a). Three dimensional representation of the distribution of material, (4004 explosions), in run c of the case with D=0.8, f=0.02. The surfaces in this figure represent the shells of explosions. In the interior of these shells we would find voids. This illustration cannot be distinguished from a random distribution. b). The 2491 members of the largest interconnected network.

Figure 3:

The curve $\log N(r)$ vs. $\log r$ for run c of the case D=0.8, f=0.02. The slope of this curve is d_f=3+γ. The increasing slope at smaller separations is typical of most cases.

Figure 4 a,b,c:

The slope of the correlation function, γ, in all ranges of r in which it is constant, for all cases in runs a, b and c respectively. The solid lines signify a relatively constant slope in that range and dotted lines indicate a

changing slope.

Figure 5:

γ's in the smallest separation ranges, (the solid portions at the far left of Figures 4 a,b and c), are compared between all cases. γ can be as low as $\sim$ -1.8 at intermediate values of D.

Figure 6:

The distribution of material in run a of the case D=0.75, f=0.01. As in Figure 2a, there is no non-random structure readily apparent.

Figure 7 a,b,c:

The curves $\log N(r)$ vs. $\log r$ for runs a,b, and c of the case with D=0.85, f=0.0005. There is an unusual trend of a decreasing slope as the separation increases, particularly in c.

Figure 8:

The distribution of material in run c of the case D=0.85, f=0.0005. Two large separate structures are apparent as well as several small structures. This indicates that large scale structure has been generated. Contrast this diagram with Figure 2a.

Authors' Address

Jane C. Charlton and David N. Schramm

Astronomy and Astrophysics Center

5640 S. Ellis Ave.

Chicago, Il. 60637

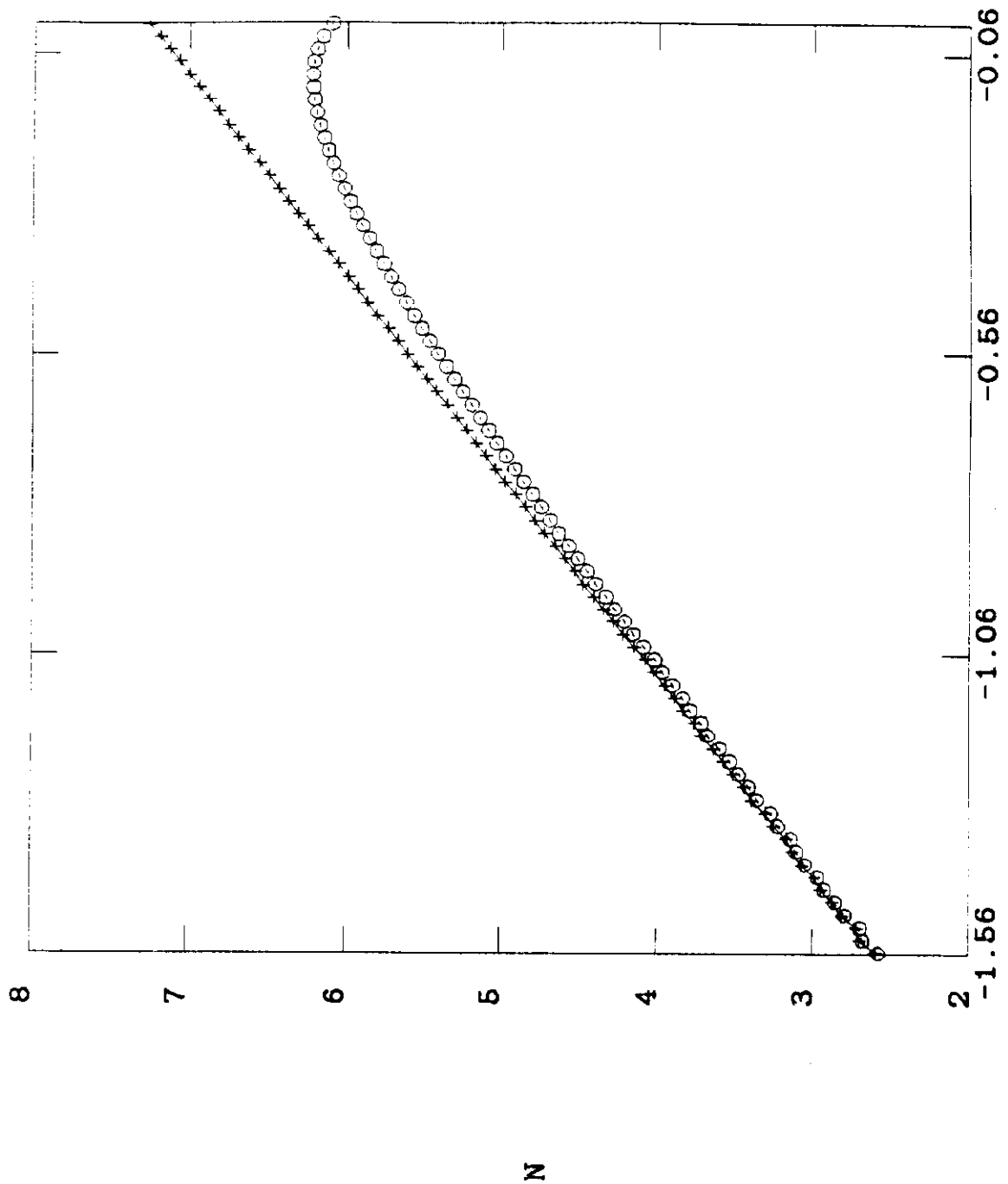

FIGURE 1

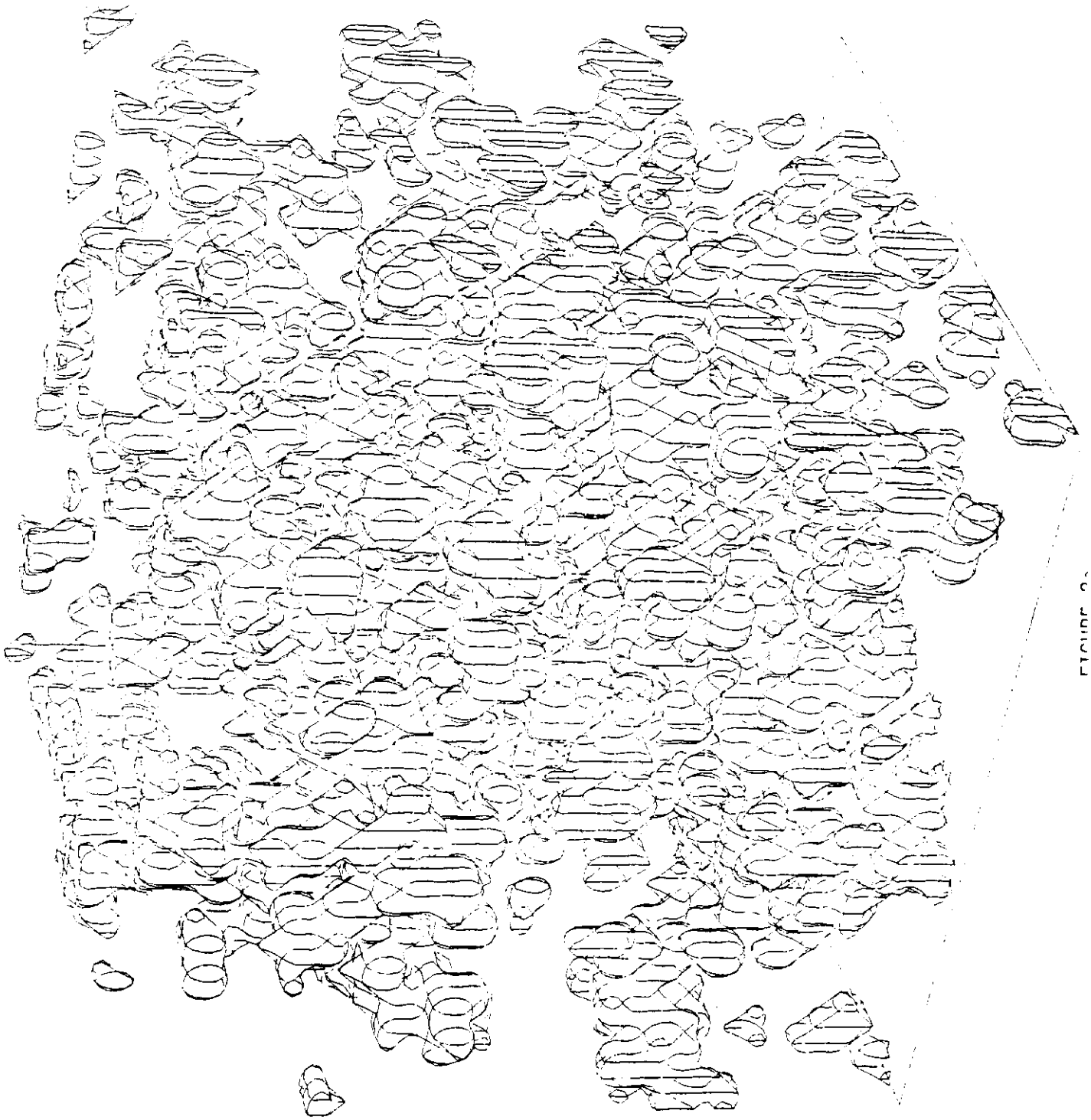

FIGURE 2A

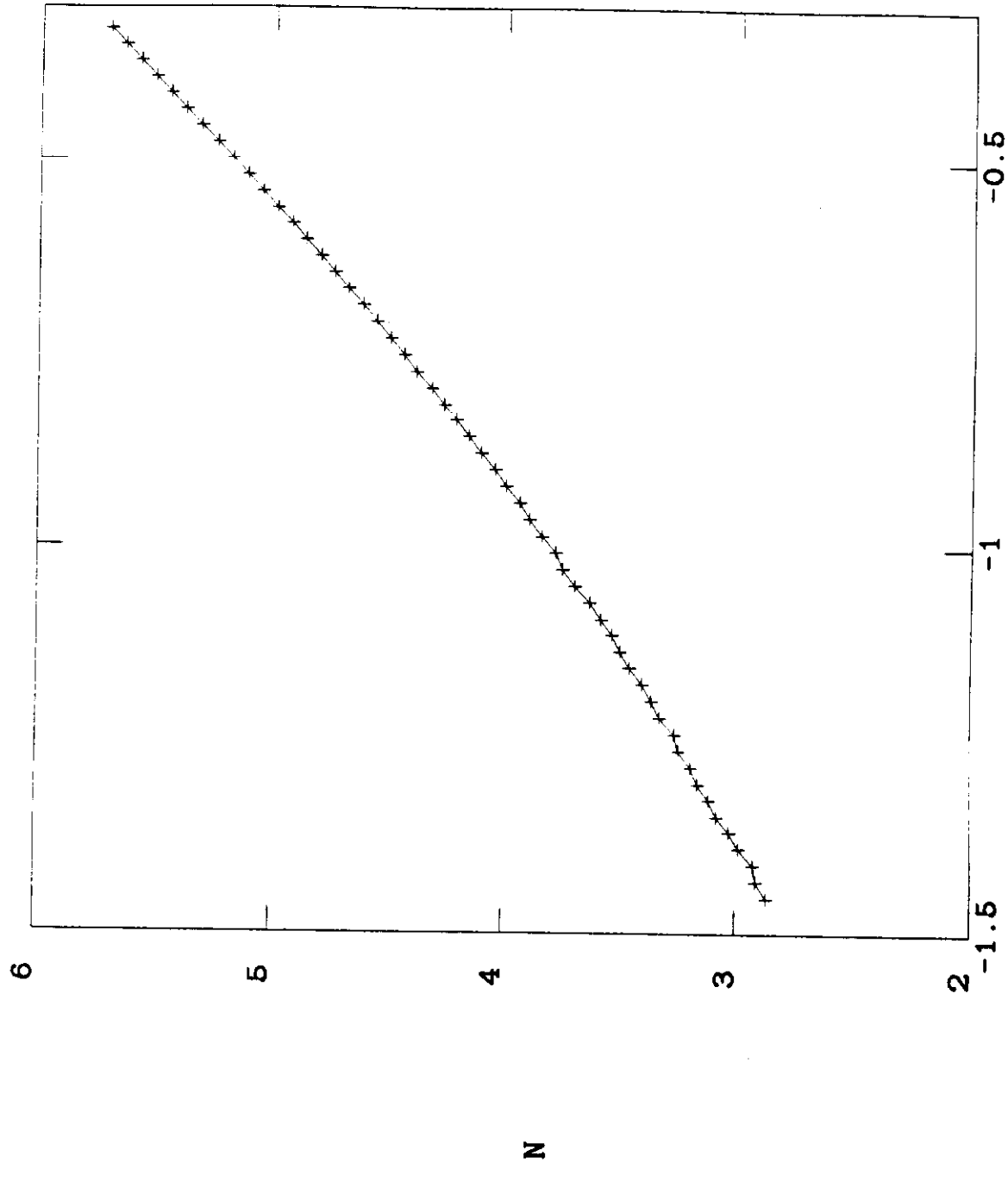

FIGURE 3

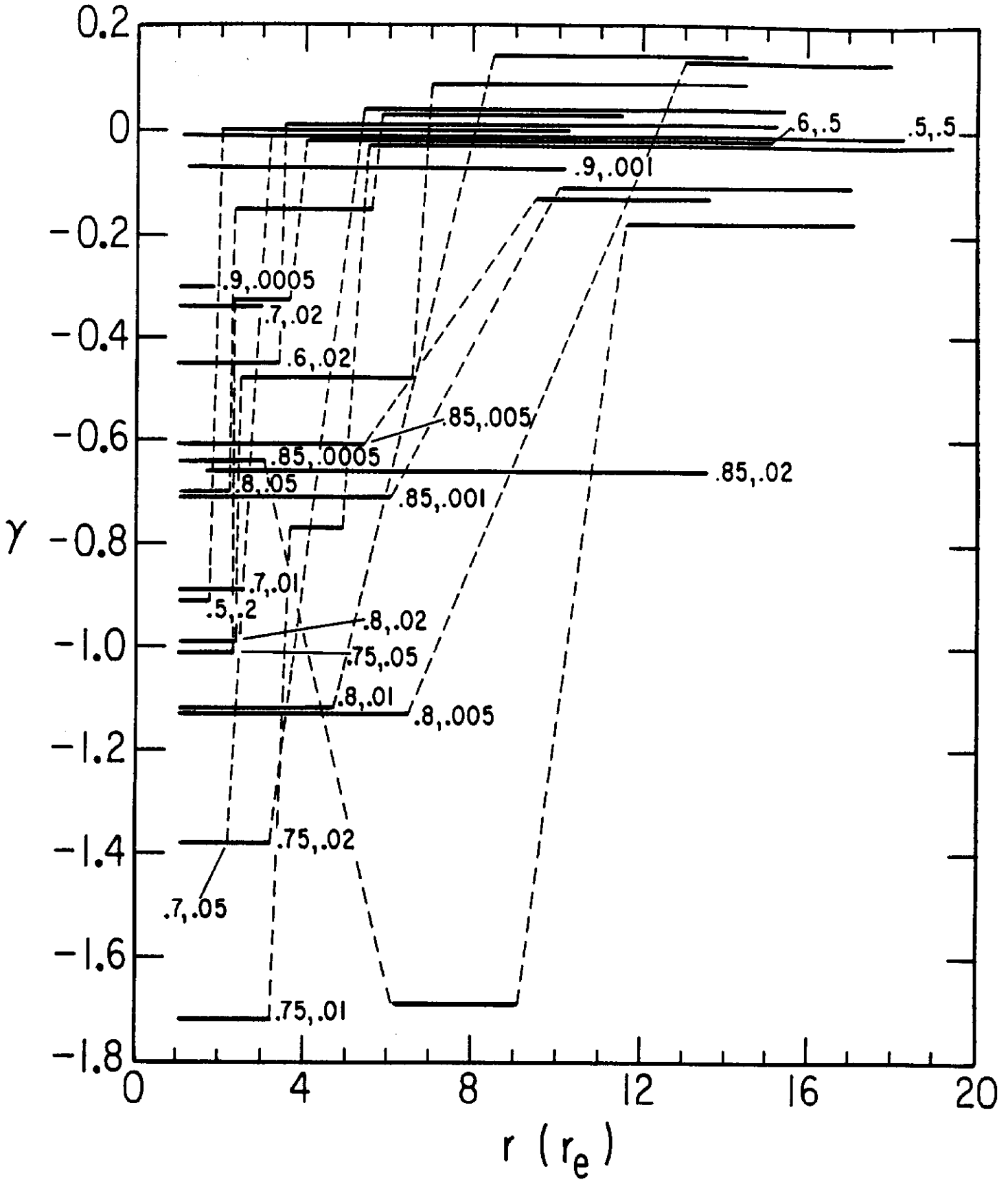
0.2
0
-0.2
-0.4
-0.6
-0.8
-1.0
-1.2
-1.4
-1.6
-1.8
γ
0
4
8
12
16
20
r (r_e)
.6,.5
.5,.5
.9,.001
.9,.0005
.7,.02
.6,.02
.85,.005
.85,.0005
.85,.02
.8,.05
.85,.001
.7,.01
.5,.2
.8,.02
.75,.05
.8,.01
.8,.005
.75,.02
.7,.05
.75,.01

FIGURE 4a

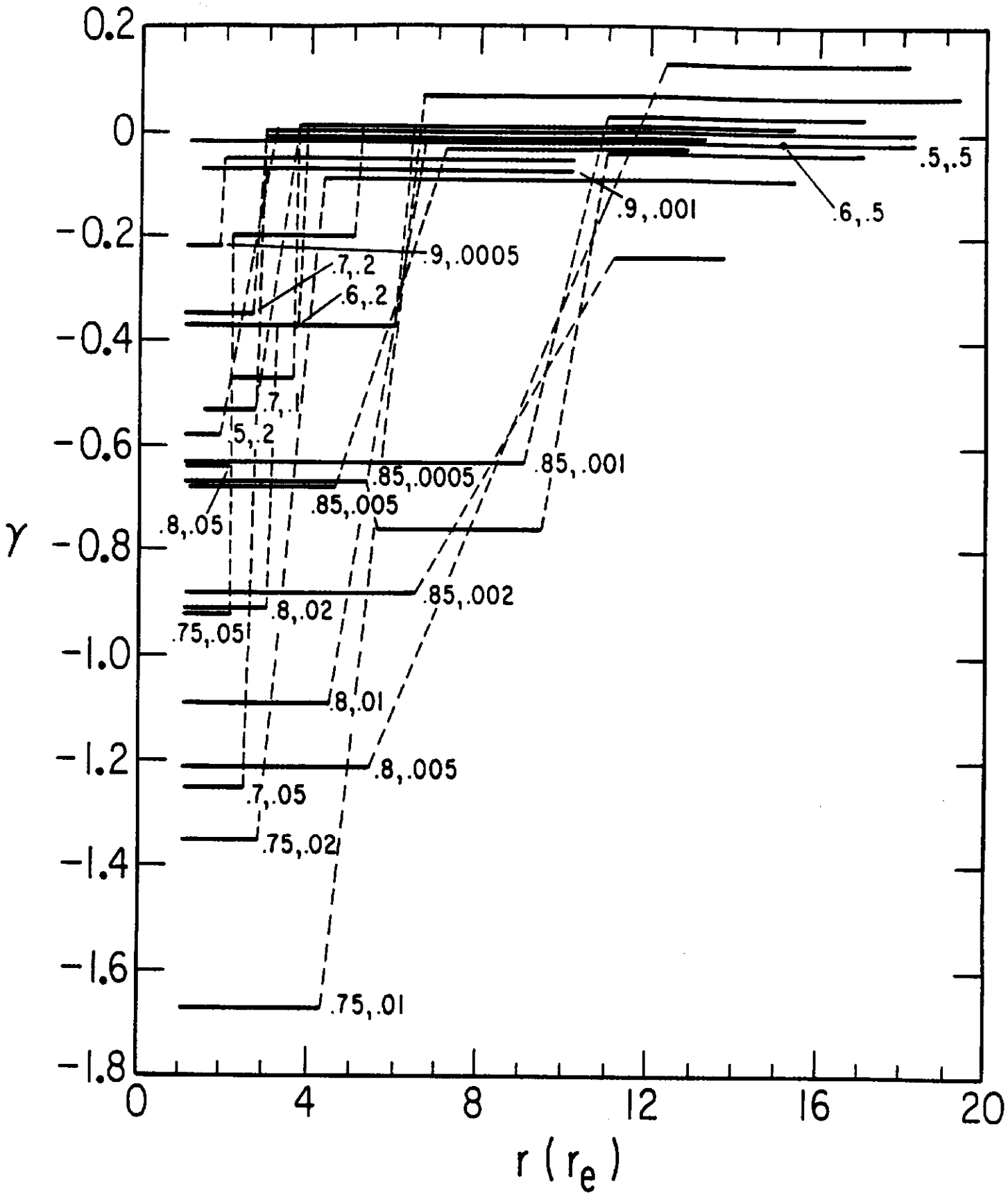
0.2
0
-0.2
-0.4
-0.6
-0.8
-1.0
-1.2
-1.4
-1.6
-1.8
γ
0
4
8
12
16
20
r (r_e)
.5,.5
.6,.5
.9,.001
.9,.0005
.7,.2
.6,.2
.7,.1
.5,.2
.85,.0005
.85,.001
.85,.005
.8,.05
.85,.002
.8,.02
.75,.05
.8,.01
.8,.005
.7,.05
.75,.02
.75,.01

FIGURE 4b

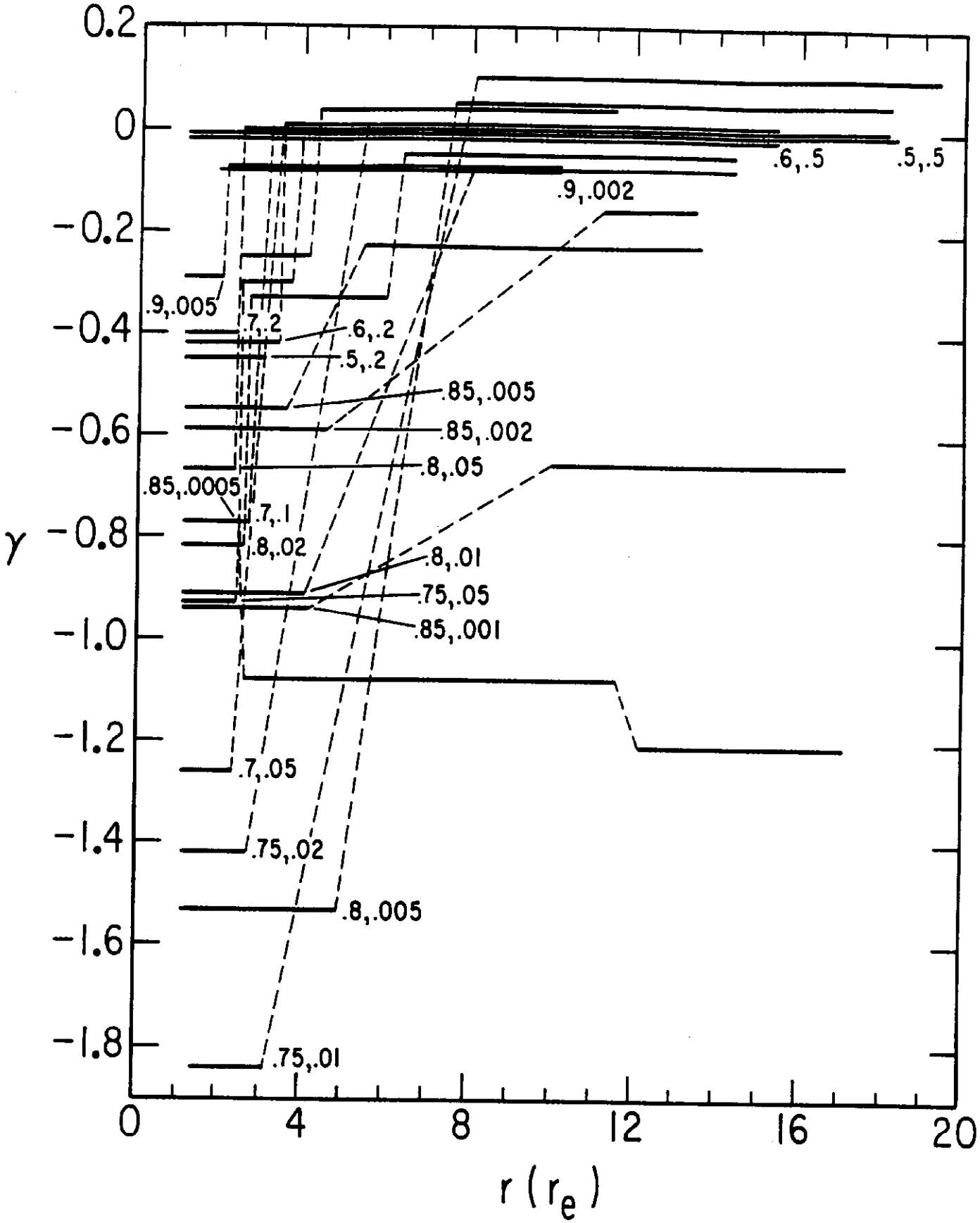
0.2
0
-0.2
-0.4
-0.6
-0.8
-1.0
-1.2
-1.4
-1.6
-1.8
γ
0
4
8
12
16
20
r (r_e)
.6,.5
.5,.5
.9,.002
.9,.005
.7,.2
.6,.2
.5,.2
.85,.005
.85,.002
.8,.05
.85,.0005
.7,.1
.8,.02
.8,.01
.75,.05
.85,.001
.7,.05
.75,.02
.8,.005
.75,.01

FIGURE 4c

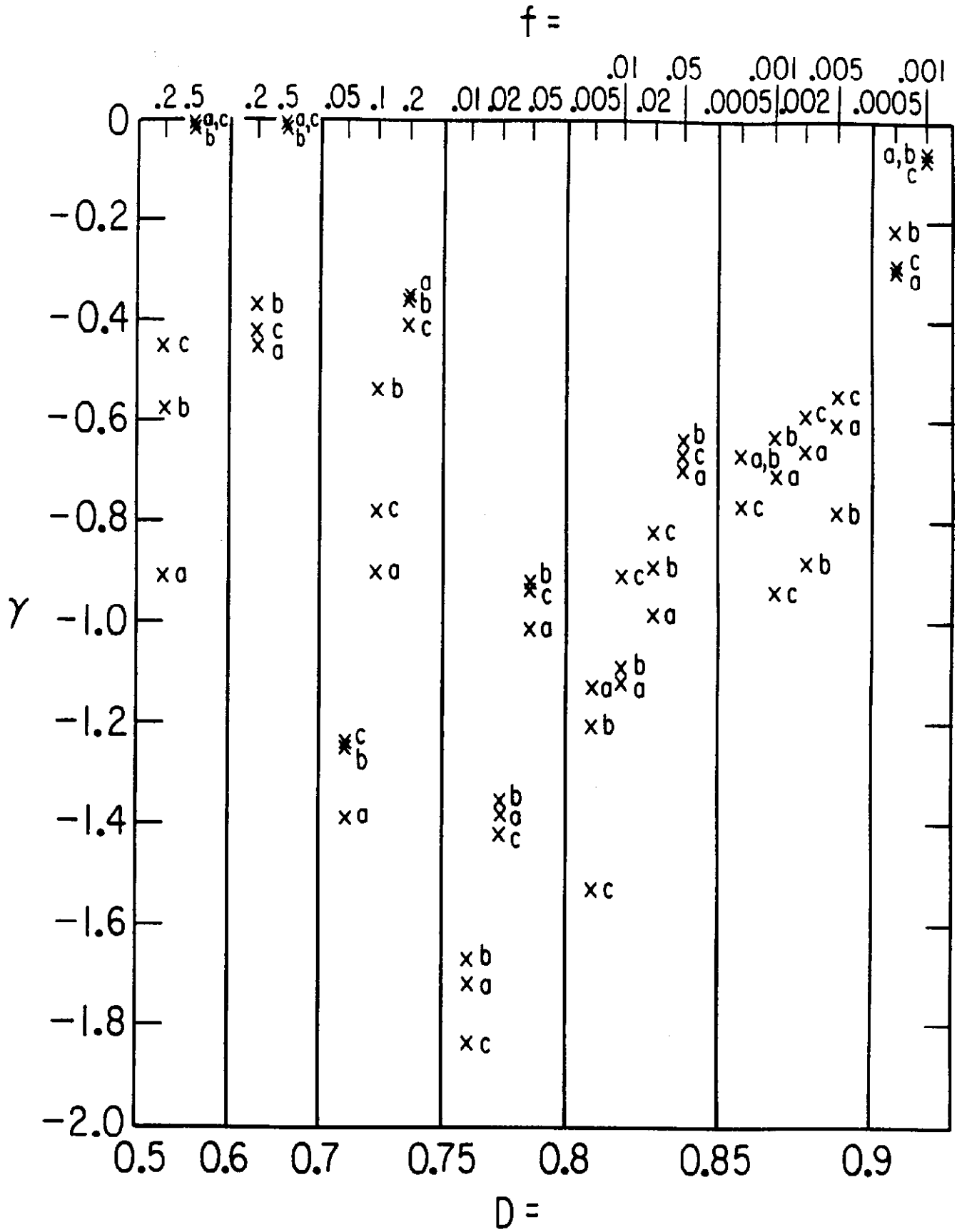
f =
.2 .5 .2 .5 .05 .1 .2 .01 .02 .05 .005 .01 .05 .02 .001 .005 .001 .0005 .002 .0005
0
-0.2
-0.4
-0.6
-0.8
-1.0
-1.2
-1.4
-1.6
-1.8
-2.0
γ
0.5 0.6 0.7 0.75 0.8 0.85 0.9
D =

FIGURE 5

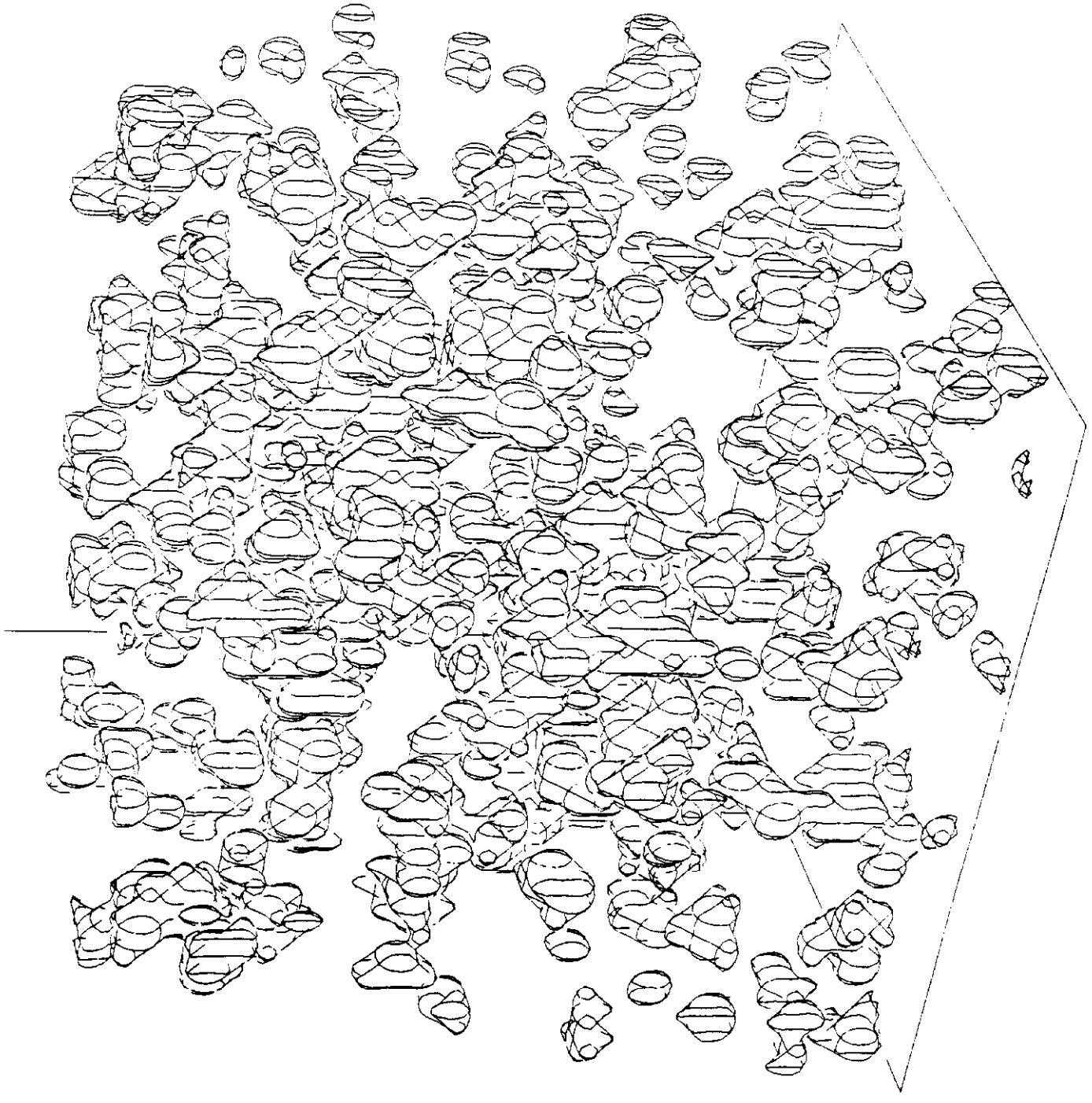

FIGURE 6

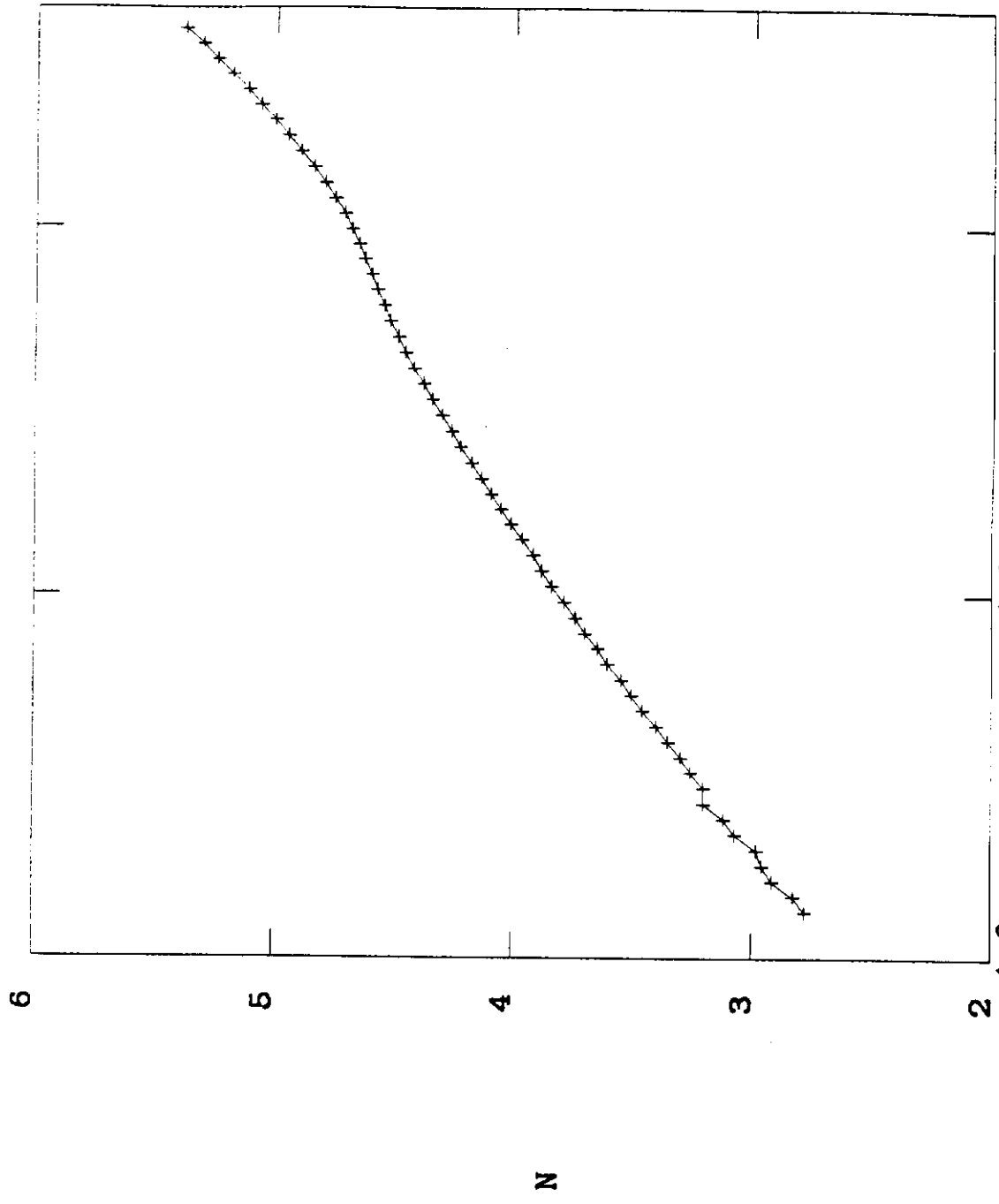

FIGURE 7a

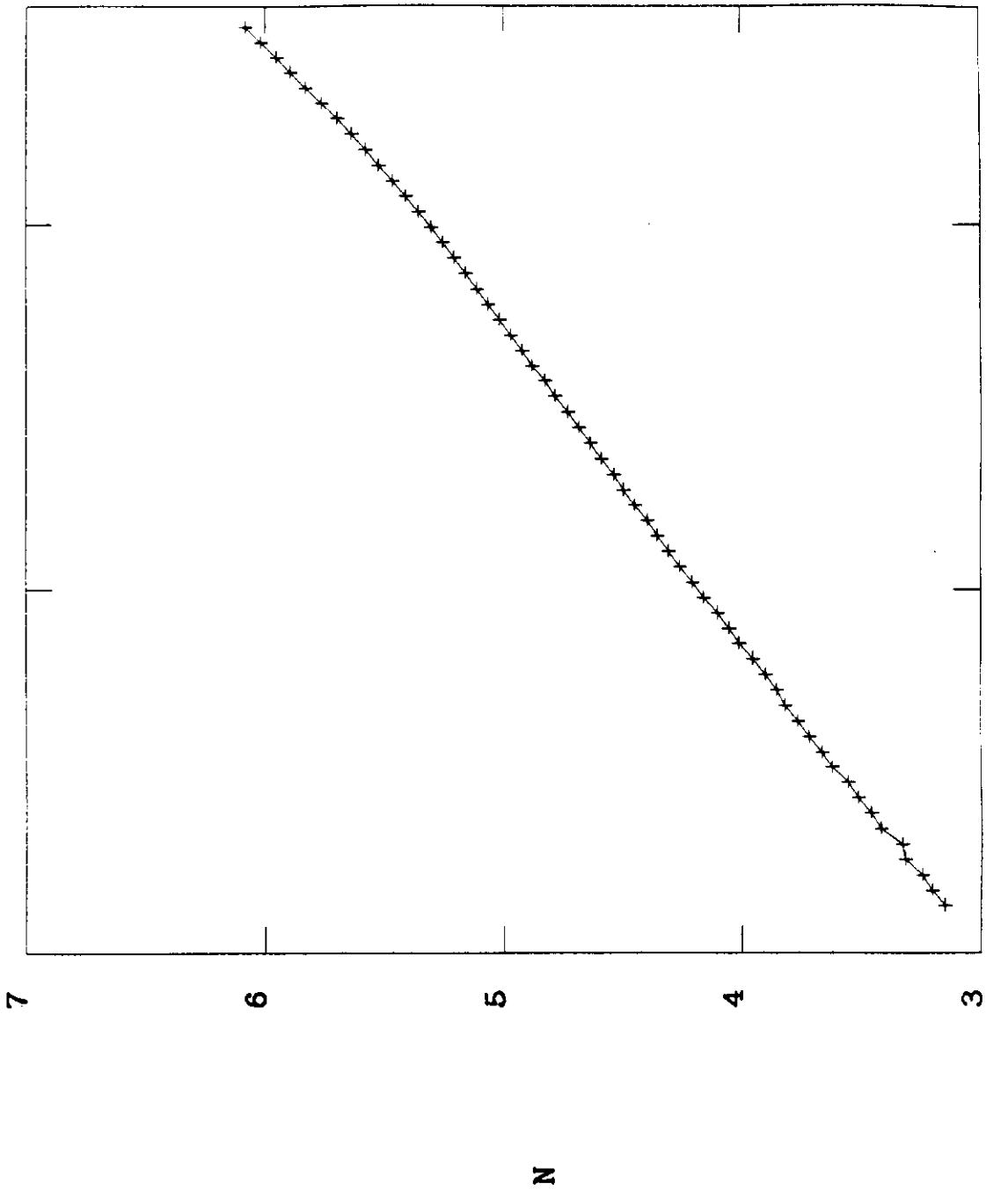

FIGURE 7b

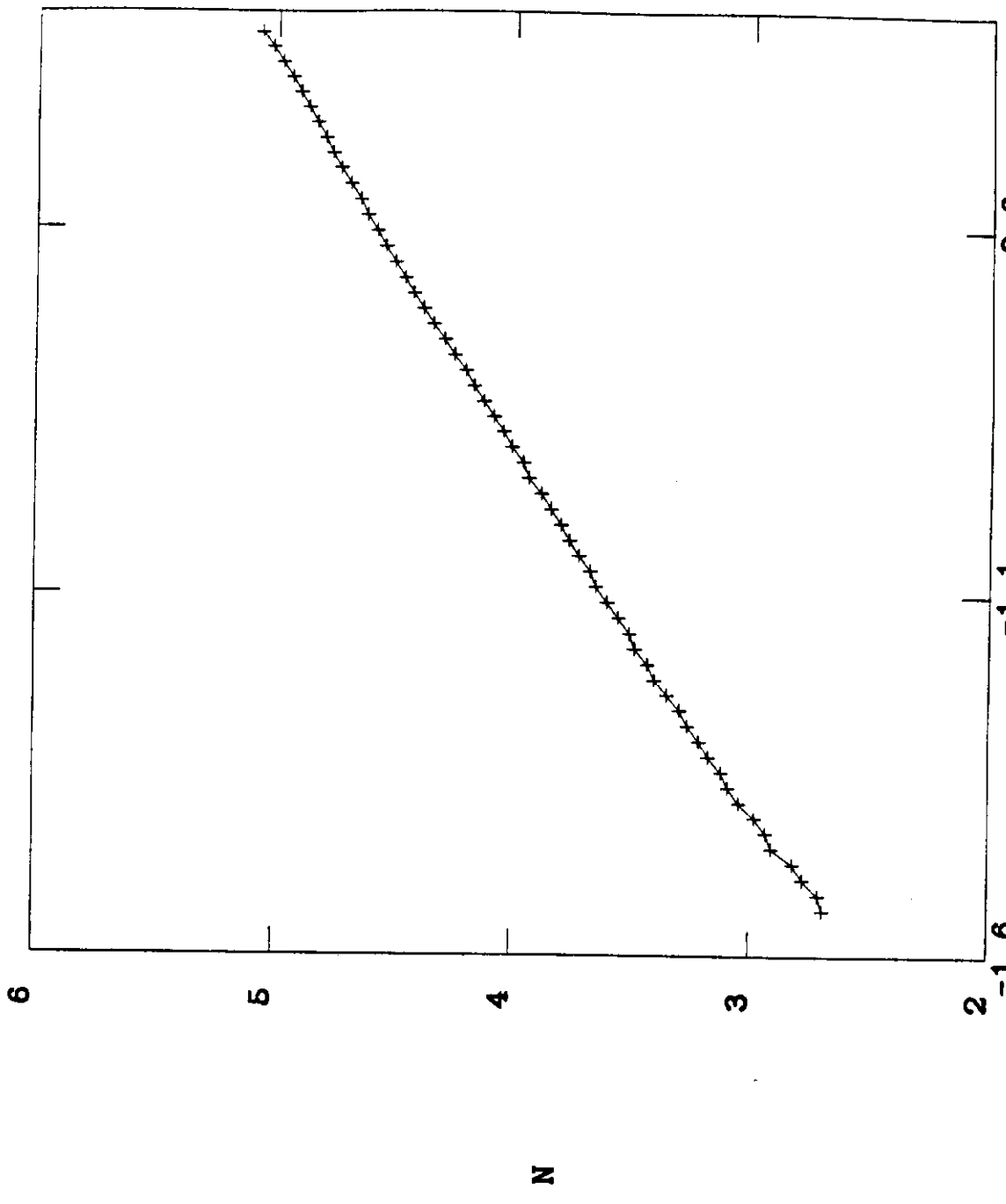

FIGURE 7c